Effects of Precursor Structure and the Content of the SO_4^{2-} on the Electrochemical Performance of $LiNi_xCo_yMn_{1-x-y}O_2$ Cathode Materials

Yan Cui*, Qiang Fu

China National Institute of Standardization, No. 4 Zhichun Road, Beijing, China

*Corresponding author e-mail: cuiyan@cnis.gov.cn

Abstract. In the present work, the effects of the SO_4^{2-} content, the crystal growth pattern, the agglomeration of the primary particle on the electrochemical performance are first studied systematically. The $LiNi_{0.4}Co_{0.2}Mn_{0.4}O_2$ precursors are obtained by the controlled crystallization method by different conditions. But the larger primary particle is not beneficial to its electrochemical performances. All the conclusions show that sample 2 possesses the best electrochemical performances, including high capacity, excellent cycle properties. The initial specific capacity at 1C rate of sample 2 is 145.2 mAh/g operated between 4.3and 2.7 V, and 99.4% capacity is maintained after 50 cycles.

1. Introduction

In recent years, the lithium ion battery (LIB) is one of the most important rechargeable energy storage technologies, and can be used for a variety of mobile applications, including cell phones, laptop computers, and power tools. It is also a promising candidate for powering electric vehicles [1–2]. However, a challenge for new generation lithium-ion batteries is to develop new cathode materials to replace the currently used material such as $LiCoO_2$, which is expensive, toxic [3-4]. $LiNi_xCo_yMn_{1-x-y}O_2$ (NCM) provides higher battery capacity in a wider voltage range, and shows better safety characteristics than conventional $LiCoO_2$. It is well known that the performance of the powders used as cathode materials in lithium-ion batteries is strongly affected by their preparation processes, thus indicating how important it is to select a suitable method to prepare high-performance Li $[Co_{1/3}Ni_{1/3}Mn_{1/3}]O_2$. Various new techniques, such as glycine-nitrate combustion, hydroxide co-precipitation, carbonate co-precipitation, ultrasonic spray pyrolysis, and sol–gel processes have been developed for preparing high-quality Li $[Co_{1/3}Ni_{1/3}Mn_{1/3}]$ O_2. [5-9] Although some NCM compounds, such as $Li[Ni_{0.5}Co_{0.2}Mn_{0.3}]O_2$, $Li[Ni_{0.4}Co_{0.2}Mn_{0.4}]O_2$, Li $[Ni_{1/3}Co_{1/3}Mn_{1/3}]O_2$, have been successfully commercialized, the properties of the precursor on the physical properties and the final electrochemical performance of NCM are not yet well understood. In the present work, the effects of crystal form, the SO_4^{2-} content, the crystal growth pattern, the agglomeration of the primary particle are studied systematically. In order to study the properties of the NCM precursor, a series of $Ni_{0.4}Co_{0.2}Mn_{0.4}(OH)_2$ precursors were prepared by the co-precipitation at different conditions. In this paper, $Ni_{0.4}Co_{0.2}Mn_{0.4}(OH)_2$ is used as the basic material to study, but it is believed that the conclusions are applicable to all the NCM materials.

2. Experiment procedures

2.1. Sample preparation

To prepared $LiNi_{0.4}Co_{0.2}Mn_{0.4}O_2$ powders, stoichiometric amounts of the as-prepared $Ni_{0.4}Co_{0.2}Mn_{0.4}(OH)_2$ and Li_2CO_3 were mixed, and then sintered at 900°C for 15h. The both powders are labelled as sample 1 and sample 2.

2.2. Powder X-ray diffraction and scanning electron microscope

The structure of $LiNi_{1/3}Co_{1/3}Mn_{1/3}O_2$ material was determined by X-ray diffraction (XRD, Rigaku, RU-200). The scan data were collected in the 2θ range of 10–80º in steps of 2° per minute. The particle size and morphological features of the obtained powders were observed *via* a scanning electron microscope equipped with Energy Dispersive Spectroscopy (EDS).

The charge and discharge behaviors were investigated using CR2032-type coin cells. The cathode composite was prepared by mixing active material, acetylene black and polytetrafluoroethylene (PTFE) binder in the weight ratio of 80:10:10. The mixture was rolled into thin sheets. The sheets were cut into roundels of 6 mm in diameter.

3. Results and discussion

*3.1. **X**-ray diffraction*

The crystal structures of the precursors were evaluated by XRD. The two precursors prepared by different conditions showed different XRD patterns. The strongest XRD peak of Fig.1 (a) defines as (110), and it locates at about 10 degree. However, the strongest XRD peak of Fig.1 (b) defines as (001), and it locates at about 20 degree. In addition, the XRD patterns in Fig.1 (b) is the same as the references, all diffraction lines are indexed to a hexagonal structure with a space group of P -3 m1. So theoretically, the structure of the primary particle should belong to hexagonal structure, the schematic diagram is shown in Fig. 2. In crystal category, the XRD pattern can reflect the crystal growth direction. The crystal face of (001) has the strongest diffraction intensity, it indicates that the $Ni_{0.4}Co_{0.2}Mn_{0.4}$ $(OH)_2$ crystal grows mainly along the c axis. So it can speculate that the thickness along the c axis of the primary particle could be thicker. In other word, the value of d_c should be higher. The conclusion is consistent with the SEM results which will be discussed in the follow section. The clearly split (0 0 6, 0 1 2) and (0 1 8, 1 1 0) pairs in the XRD patterns indicate that the layered structure is formed. On the other hand, *c*/*a* value of the sample is more than 4.9, which is desirable for better hexagonal structure. The refined cell parameters for the sample are a =2.8639 and c = 14.1958. The refined cell parameters are approximately equal to those of the standard $LiNi_{0.4}Co_{0.2}Mn_{0.4}O_2$. The integrated intensity ratio of the (0 0 3) to (1 0 4) lines in the XRD patterns was shown to be a measure of the cation mixing. When I003/I104>1.2, the degree of cation mixing is smaller. The integrated intensity ratio of (003) to (104) peaks of this sample is above 1.2, indicating lower amount of cation mixing.

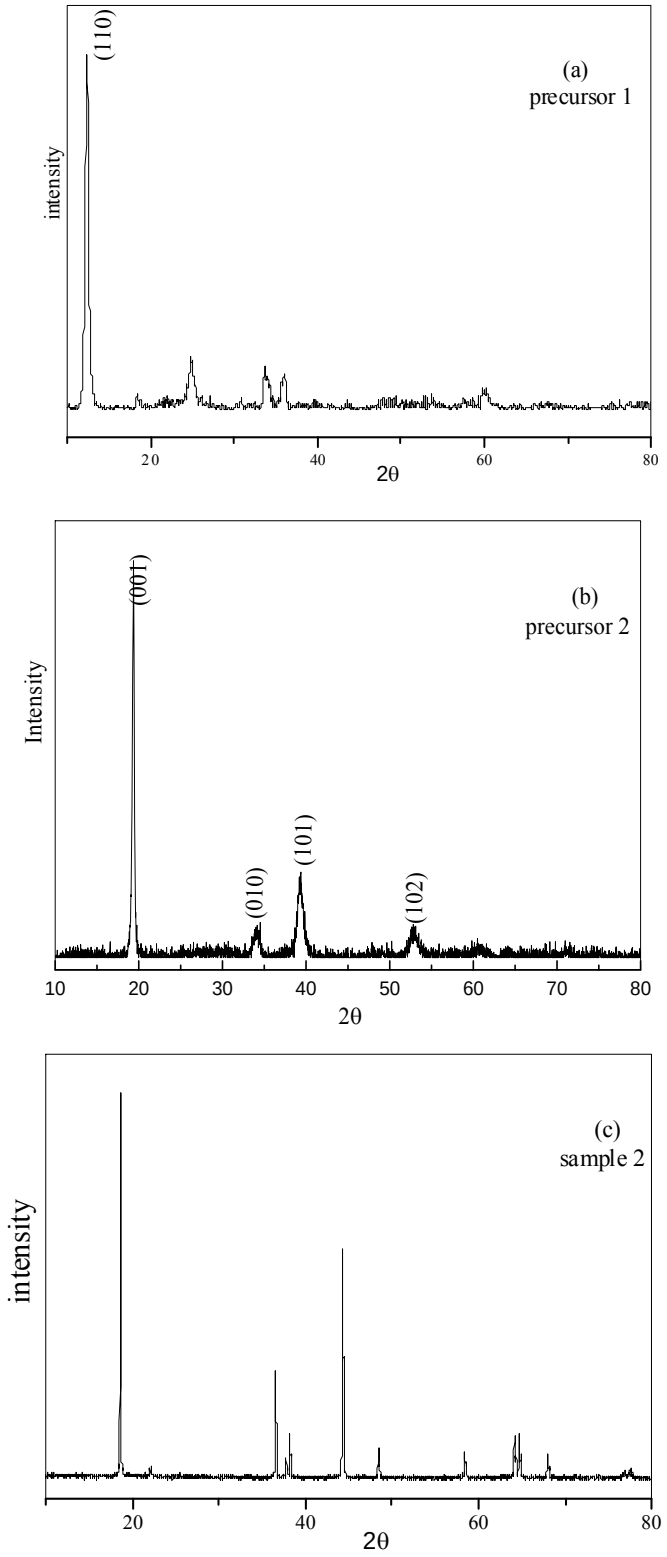

Fig 1. XRD patterns of the precursors and samples

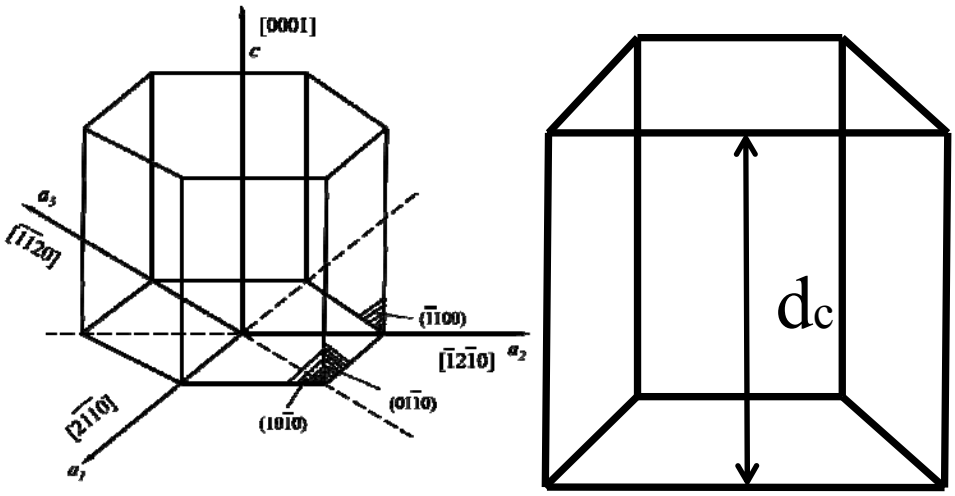

Fig 2. The schematic diagram of hexagonal structure

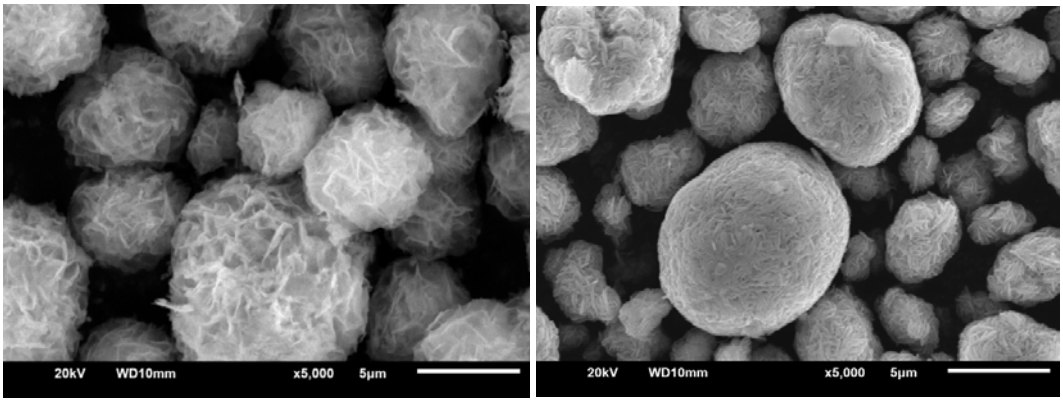

(a) (b)

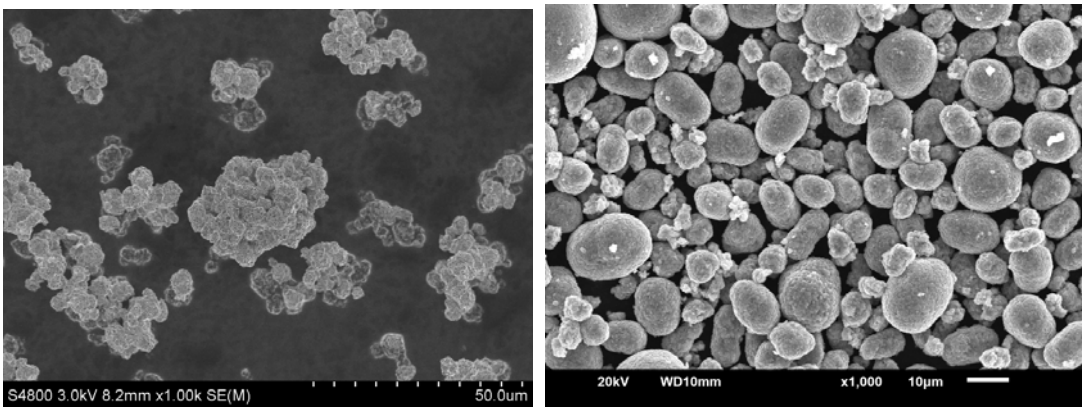

(c) (d)

Fig 3. The SEM images of $Ni_{0.4}Co_{0.2}Mn_{0.4}(OH)_2$ precursors and $LiNi_{0.4}Co_{0.2}Mn_{0.4}O_2$ samples

3.2. Surface morphology

The SEM images of $Ni_{0.4}Co_{0.2}Mn_{0.4}(OH)_2$ precursors and $LiNi_{0.4}Co_{0.2}Mn_{0.4}O_2$ samples are shown in Fig. 3. As shown in all SEM images, the secondary particles are composed of aggregated primary particles. From the images, it can be seen that the morphology of the particles is spherical. From the

SEM images (a)-(b), it can be seen that the primary particles are obviously distinguished between precursor 1 and precursor 2. Theoretically, the structure of the primary particle should belong to hexagonal structure, just as shown in the schematic diagram of Fig 2. In Fig.3 (a), the primary particle of precursor 1 aggregate more loose than that of precursor 2 as shown in Fig.3 (b). The particles of precursor 1 are porous and the tap density is much lower than that of precursor 2. The tap density of precursor 1 is 1.1g/cm^3, while the tap density of precursor 2 is 2.05g/cm^3. The morphology of the primary particles of precursor 1 is a distorted hexahedron, and the dc of the hexahedron is difficult to measure accurately. It is indicated from the XRD data that the NiCoMn (OH) $_2$ crystal grows mainly along the (110) crystal face. So the hexagonal structure is twisted accompanied the growth process. On the other hand, the primary particles aggregate compactly, so secondary particles of precursor 2 represents a porousless spherical structure.

The $LiNi_{0.4}Co_{0.2}Mn_{0.4}O_2$ powders were obtained by sintering $Ni_{0.4}Co_{0.2}Mn_{0.4}(OH)_2$ and Li_2CO_3 at 900°C for 15h, and the SEM images are shown in Fig.3(c)-(d). It is indicated that the secondary particles are aggregated apparently together. However, the particles of sample 2 disperse independently in the scope of SEM view.

3.3. ICP analysis

Table 1. The data of ICP for sample 1 and sample 2

Number	**Total element content wt%**	**Ni wt%**	**Mn wt%**	**Co wt%**	**Na wt%**	**Fe wt%**	**Cu wt%**	**Zn wt%**	**Al wt%**	**SO_4^{2-} wt%**
Sample 1	59.21	24.31	12.38	22.52	0.0072	0.0014	0.0022	0.0003	0.0005	1.369
Sample 2	61.33	25.28	12.68	23.37	0.0054	0.0063	0.0020	0.0003	0.0005	0.2409

In order to identify the element ratios of Ni: Mn: Co for the two samples, ICP analysis is conducted. The ICP result is listed in Table 1. The result indicates that the element ratios of Ni: Mn: Co is close to 4:4:2, the total content of metal ions is 59.21% and 61.33% respectively. So total content of metal ions for sample 1 is less than that of sample 2. It is worth mentioning that there is a large SO_4^{2-} content gap between sample 1 and sample 2. The SO_4^{2-} content of sample 1 is 1.369%, while the SO_4^{2-} content of sample 2 is 0.2409%. The reason for this difference may be relate to the material structure. Due to the structure of precursor 1 is porous, it is deduced that plenty of SO_4^{2-} can hide in the pores between the primary particles, and during the washing process the hidden SO_4^{2-} cannot clean up thoroughly. As a result the SO_4^{2-} exists as impurities in the materials, and we speculate that it has an adverse effect on the electrochemical properties. The conclusion is consistence with the electrochemical performance discussed in the following section.

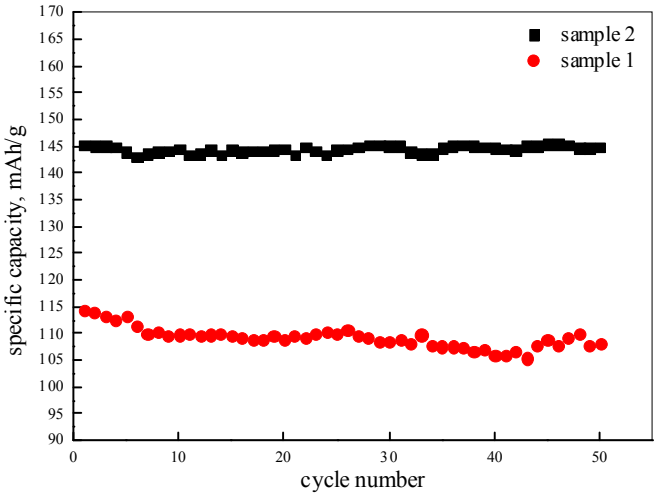

Fig4. Cycle-life performances of sample 1 and sample 2 operated between 2.7 and 4.3 V

3.4. Electrochemical performance

The cycle-life performances of sample1 and sample 2 operated between 4.3 and 2.7 V at the rate of 1C are shown in Fig4. The initial discharge capacity of sample 1is 115.1mAh/g, while the initial discharge capacity of sample 1 is 145.2mAh/g which is much higher than that of sample 1. On the other hand, the specific capacity of sample 1 decreases gradually with cycling and finally reaches 93.5% of its initial discharge capacity after 50 cycles. But the cycle performance of sample 2 is more excellent than that of sample 1 and the capacity retention is 99.4%.

As everyone knows, the structure of the materials is closely associated with the electrochemical properties. On one hand, it can be seen in Fig.3 that the primary particles of powder 1 are much larger than those of powder 2, thus the diffusion path of Li-ion of powder 1 is too longer. However, the small primary particle size can enhance the Li^+ diffusion capability due to the short diffusion path in particles. Therefor, it is rational that the specific capacity of powder 2 is better than that of powder 1. On the other hand, the higher content of SO_4^{2-} would react with the electrolyte. Few impurities can effectively prevent the fatigue of the particles during the continuously cycling and keep the structural stability. Thus, the cycle performance is prominently improved. Above all, sample 2 possesses the best electrochemical performances, including high capacity, excellent cycle properties.

4. Conclusion

In conclusion, the effects of crystal form, the SO42- content, the crystal growth patter, the agglomeration of the primary particle on the electrochemical performance are first studied systematically. SEM images show that the morphology of the particles is spherical and particle size distribution is located from 2 to 20 μm. It is indicated that the SO42- exists as impurities in the materials, and it has an adverse effect on the electrochemical properties. The primary particles of sample 2 aggregate compactly, and it represents a porousless spherical structure. Sample 2 possesses the best electrochemical performances, including high capacity, excellent cycle properties.

References

[1] Longwei Liang, Ke Du, Zhongdong Peng, Co–precipitation synthesis of $Ni_{0.6}Co_{0.2}Mn_{0.2}(OH)_2$ precursor and characterization of $LiNi_{0.6}Co_{0.2}Mn_{0.2}O_2$ cathode material for secondary lithium batteries, Electrochimica Acta 130 (2014) 82–89

[2] Chang Z. R, Chen Z. J, Wu F, "Synthesis and characterization of high-density non-spherical Li (Ni1/3Co1/3Mn1/3)O2 cathode material for lithium ion batteries by two-step drying method", Electrochimica Acta, 53 (2008)5927–5933

[3] Zhongling Xu , Lingli Xiao , Fei Wang, *et al*, Effects of precursor, synthesis time and synthesis

temperature on thephysical and electrochemical properties of Li (Ni1-x-yCoxMny)O2 cathode materials,Journal of Power Sources, 248 (2014) 180-189

[4] Cho, T. H, Park, S. M, & Yoshio, M. Preparation of layered Li [Ni1/3Mn1/3Co1/3] O2 as a cathode for lithium secondary battery by carbonate coprecipitation method. Chemistry Letters, 33 (2004) 704–705

[5] Zhang S, Deng C, Fu B.L, "Synthetic optimization of spherical Li ($Ni_{1/3}Co_{1/3}Mn_{1/3}$)O_2 prepared by a carbonate co-precipitation method", *Powder Technology*, 198 (2010)373–380

[6] Sebastien P, Marca M. D, "Direct synthesis of Li($Ni_{1/3}Co_{1/3}Mn_{1/3}$)O_2 from nitrate precursors", Electrochemistry Communications, 6(2004)767–772

[7] Patoux, S, &Doeff, M. M. Direct synthesis of $LiNi_{1/3}Co_{1/3}Mn_{1/3}O_2$ from nitrate precursors. Electrochemistry Communications, 6, (2004) 767–772.

[8] Park, S.H, Yoon, C. S, Kang, S.G, Kim, H. -S, Moon, S.-I, &Sun, Y.-K. Synthesis and structural characterization of layered Li [Ni1/3Co1/3Mn1/3] O 2 cathode mate-rials by ultrasonic spray pyrolysis method. Electrochimica Acta, 49 (2004) 557–563.

[9] Hwang, B. J, Tsai, Y. W., Carlier, D., & Ceder, G. A combined computational/experimental study on $LiNi_{1/3}Co_{1/3}Mn_{1/3}O_2$. Chemistry of Materials, 15 (2003)3676–3682.